



## Improving tribological behavior of friction stir processed A413/SiC<sub>p</sub> surface composite using MoS<sub>2</sub> lubricant particles

M. JANBOZORGI<sup>1</sup>, M. SHAMANIAN<sup>2</sup>, M. SADEGHIAN<sup>1</sup>, P. SEPEHRINIA<sup>2</sup>

1. Department of Materials Science and Engineering, Sharif University of Technology, Tehran 1136511155, Iran;

2. Department of Materials Science and Engineering, Isfahan University of Technology, Isfahan 8415683111, Iran

Received 17 February 2016; accepted 19 September 2016

**Abstract:** The effect of MoS<sub>2</sub> lubricant particles on the microstructure, microhardness and tribological behavior of A413/SiC<sub>p</sub> surface composite, fabricated via friction stir processing (FSP), was studied. For this purpose, the FSP was carried out with tool rotational speed of 1600 r/min, tool travel speed of 25 mm/min and tool tilt angle of 3° through only a “single pass”. The optical and scanning electron microscopies, microhardness and reciprocating wear tests were used to characterize the samples. The results showed that the addition of MoS<sub>2</sub> lubricant particles to A413/SiC<sub>p</sub> surface composite leads to the decrease of friction coefficient and mass loss. In fact, the generation of mechanically mixed layer (MML) containing MoS<sub>2</sub> lubricant particles in A413/SiC<sub>p</sub>/MoS<sub>2p</sub> surface hybrid composite results in the reduction of metal-to-metal contact and subsequently leads to the improvement of tribological behavior.

**Key words:** friction stir processing; surface hybrid composite; microstructure; microhardness; tribological behavior

### 1 Introduction

A specific feature involving high specific strength of cast Al–Si alloys leads to the decrease of fuel consumption and increase of mechanical performance of these alloys in the engineering industries [1]. A413 cast Al–Si alloy (with 11%–13% Si, mass fraction) is widely used in the engine components such as pistons, housings, connecting rods, marine fittings and water manifolds because of excellent castability, good dimensional stability and high corrosion resistance [2]. However, the high silicon content in this alloy results in the superior casting characteristics, low shrinkage and poor machining [1]. MAHMOUD and MOHAMED [2] reported that A413 cast Al–Si alloy is characterized by various defects like casting porosities and silicon flakes which limit the using of this alloy in many applications. They used the friction stir process (FSP) to eliminate the casting porosities and to break the silicon flakes.

The FSP as a new solid state technique, based on the friction stir welding (FSW), can be used to the development of microstructural refinement and fabrication of surface composites. MISHRA and MA [3] developed the FSP technique in which a non-consumable

tool, with a specially designed pin and shoulder, inserted into the groove which was machined out of workpiece and was filled with powders. This tool then rotates around the own axis and traverses along the surface groove. Figure 1 shows the schematic drawing of FSP setup. In addition, the FSP is known as a metal forming process including forging and extrusion [4]. In fact, during the FSP, the metal is exposed to intense plastic deformation and high frictional heating which results in softening the material around the pin. Then the combination of tool rotation and tool translation leads to the movement of material from the front of pin to the back of pin [3]. As a result of this process, a surface composite is produced in the “solid state” because the FSP is carried out at the temperature below the melting point of substrate. The mechanical properties and tribological behavior of this surface composite are better than that of the base metal.

The excellent mechanical properties and tribological behavior of metal matrix composites (MMCs), where hard ceramic particles have been distributed in a relatively ductile matrix, lead to the widespread applications of these composites in the engineering industries [5]. Several investigations have shown that the addition of reinforcement particles such as SiC and

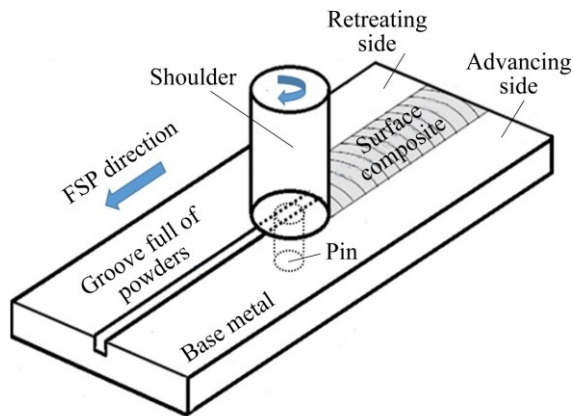


**Fig. 1** Schematic drawing of FSP setup

$\text{Al}_2\text{O}_3$  into the matrix of Al alloys using FSP, leads to the improvement of mechanical properties and tribological behavior of Al alloys [5–7]. However, these hard reinforcement particles increase the wear rate and mass loss of counter faces, and change the wear mechanism and tribological behavior of contact surfaces because of detaching from the matrix and acting as third-body abrasives in the wear [8]. Recent investigations have shown that the addition of lubricant particles such as  $\text{MoS}_2$  and graphite together reinforcement particles such as SiC and  $\text{Al}_2\text{O}_3$  into the matrix of Al alloys using FSP, leads to further improvement of tribological behavior of Al alloys [8–10].

In this research, A413/SiC<sub>p</sub>/MoS<sub>2p</sub> surface hybrid composite was produced using FSP as a novel research. The mechanical properties and tribological behavior of this surface hybrid composite were evaluated and the microstructural changes were observed.

## 2 Experimental

The material used in this research was A413 cast Al–Si alloy plate with dimensions of 8 mm × 60 mm × 80 mm. The chemical composition of the alloy was given in Table 1. The reinforcement particles of SiC (purity of 99.5% and average particle size of 7 μm) and lubricant particles of  $\text{MoS}_2$  (purity of 99% and average particle size of 10 μm) were used to fabricate the surface composites. The FSP tool was made of hardened H-13 tool steel and had a columnar shape with a shoulder (diameter: 16 mm, height: 68 mm) and a pin (diameter: 6 mm, height: 3 mm).

**Table 1** Chemical composition of A413 aluminum alloy (mass fraction, %)

Si	Fe	Cu	Zn	Ni	Mn	Sn	Mg	Al
11	2	1	0.5	0.5	0.35	0.15	0.1	Bal.

A groove with depth and width of 3 and 2 mm, respectively, was machined out of the workpieces for the insertion of powders. The groove opening was initially closed by means of a pinless tool to avoid the escapement of powders from the groove during the process. Then, the FSP was performed under the rotational speed of 1600 r/min, travel speed of 25 mm/min and tilt angle of 3° through only a “single pass”. To study the effect of lubricant particles, in initial stage, SiC reinforcement particles, and then in the second stage, the mixture of (SiC<sub>p</sub>+MoS<sub>2p</sub>) with equal volume fraction were packed into the groove. As known, the main source of FSP heating is friction between tool and workpiece. In addition, the additive materials in the present work are  $\text{MoS}_2$  lubricant particles which have low friction coefficient. Consequently, using high rotational speed and low travel speed, as in the present research, leads to the increase of frictional heating and subsequently improvement of material fluidity during the FSP [2]. Moreover, the increase in rotational speed and the decrease in travel speed reduce the agglomeration of particles [11]. The angle between tool axis and workpiece normal leads to the improvement of forging action at the shoulder trailing edge [4,8].

The cross section of samples in the planes perpendicular to the FSP direction was performed for the metallographic analysis. The samples were prepared according to standard metallographic practice and etched with Keller’s reagent (2 mL HF, 3 mL HCl, 20 mL HNO<sub>3</sub> and 175 mL H<sub>2</sub>O). The optical microscope (OM) was used to characterize the microstructure of transverse section of samples.

To study the mechanical properties of samples, the Vickers microhardness test was applied. The microhardness tests were carried out with 50 g load and 15 s duration in the points with 2 mm distance from the upper surface in the transverse section.

The tribological behavior of samples was evaluated using the reciprocating wear test. Type of contact was cylinder on plate (line contact), so that the pin axis was perpendicular to the specimen surface. For the test, the plate specimens with dimensions of 8 mm × 60 mm × 60 mm were cut from the FSPed samples and the cylindrical pin with diameter of 5 mm was made from AISI 52100 steel. The reciprocation amplitude of cylindrical pin on the surface of specimen was 40 mm. The wear tests were carried out at the normal load of 15 N, sliding speed of 0.14 m/s, total sliding distance of 500 m without using a lubricant. AL-SAMARAI et al [12] showed that the wear rate and mass loss increase with increasing the normal load and decreasing the sliding speed. Therefore, high normal load and low sliding speed were used in the present research in order to provide severe condition for the wear tests of surface composites.

During the wear tests, the ranges of temperature and humidity were 20–30 °C and 40%–50%, respectively. The wear tests were interrupted at the certain intervals to determine the progress of wear. At each interval, the samples were cleaned with alcohol and mass loss was measured using a balance with an accuracy of 0.1 mg. After the wear tests, to determine the wear mechanism of samples, the worn surfaces and wear debris were examined by SEM and EDS.

### 3 Results and discussion

#### 3.1 Microstructure

Figure 2 shows the optical micrographs of cross section of A413/SiC<sub>p</sub>/MoS<sub>2p</sub> surface hybrid composite in the planes perpendicular to the FSP direction. The microstructure of base metal and FSPed regions are illustrated in Figs. 2(a) and (b), respectively. As can be seen in Fig. 2(a), the microstructure of A413 cast Al–Si alloy is mainly composed of silicon flakes and casting porosities non-homogeneously distributed along the  $\alpha$ (Al) dendrites [2]. As can be observed in Fig. 2(b), three zones can be identified in the microstructure of FSPed regions including stir zone (SZ), thermo

mechanically affected zone (TMAZ) and heat affected zone (HAZ).

According to Fig. 2, the difference between microstructure of FSPed regions and base metal is detectable. It is clear that the FSPed regions compared with the base metal exhibit a much more homogeneous microstructure. The SZ experiences intense plastic deformation and high frictional heating during the FSP and is characterized by a recrystallized fine-grained microstructure [2–4,13–15]. In the TMAZ, both heating and deformation occur during the FSP [2,3,13], which result in the generation of a highly deformed structure [2,3], including the elongated grains in the metal flow directions [16]. In addition, the increase in temperature in the TMAZ leads to facilitating the recovery processes [16]. However, MISHRA and MA [3] showed that in the TMAZ, the dissolution of some precipitation can happen due to the sufficient heating temperature, whereas, the recrystallization cannot occur owing to the insufficient deformation strain. Furthermore, the grains in the TMAZ have usually a high density of sub-boundaries [3,16]. In the HAZ, the thermal cycle occurs whereas no plastic deformation happens [3,4,13,15]. Moreover, the HAZ region has same grain structure compared with the base metal [3,4,13,15].

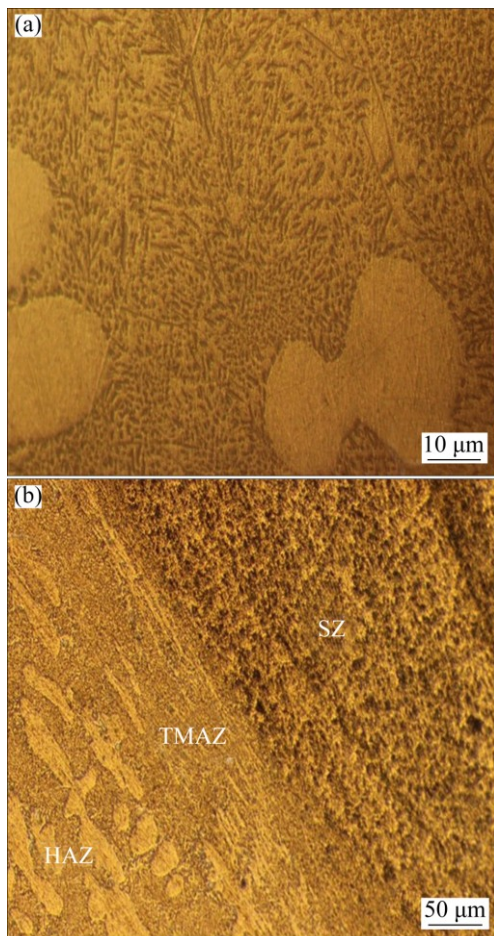


**Fig. 2** Microstructures of A413 base metal (a) and A413/SiC<sub>p</sub>/MoS<sub>2p</sub> surface hybrid composite (b)

#### 3.2 Microhardness

Figure 3 shows the microhardness profile of cross sections of A413/SiC<sub>p</sub> surface composite and A413/SiC<sub>p</sub>/MoS<sub>2p</sub> surface hybrid composite in the planes perpendicular to the FSP direction. The average microhardness of base metal is about HV 80. As can be seen in Fig. 3, the stir zone (SZ) has higher microhardness rather than the base metal (BM). This is due to the existence of SiC particles and the reduction in grain size in the SZ. This phenomenon is justifiable on Orowan mechanism and Hall–Petch relationship. According to Orowan mechanism and Hall–Petch

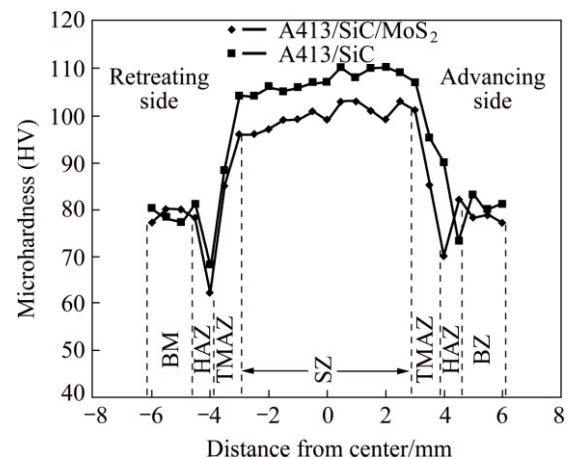


**Fig. 3** Microhardness profile of A413/SiC<sub>p</sub> surface composite and A413/SiC<sub>p</sub>/MoS<sub>2p</sub> surface hybrid composite

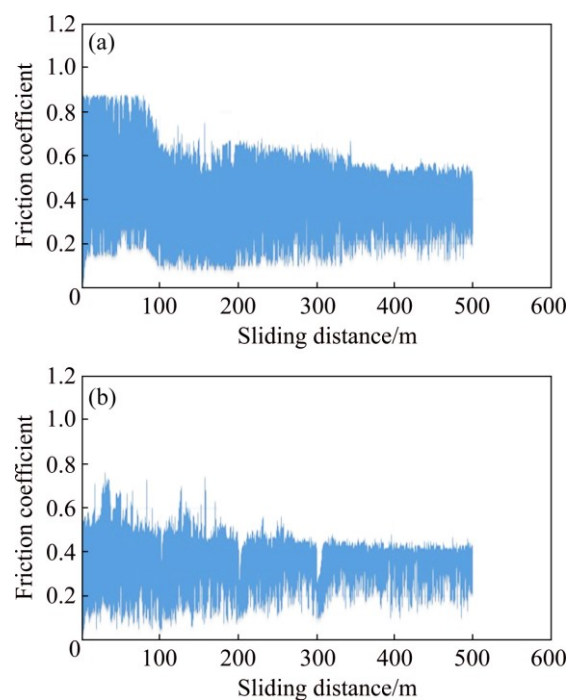
relationship, the presence of SiC particles and the decrease in grain size, respectively, lead to the increase of microhardness [10,14,16,17]. In fact, SiC particles (based on Orowan mechanism) and grain boundaries (based on Hall–Petch relationship) act as barriers in front of dislocations movement [16,17]. Therefore, the presence of SiC particles and the decrease in grain size result in a higher microhardness. Figure 3 also shows that the microhardness of TMAZ is lower than that of SZ. The decrease in microhardness in the TMAZ is due to the occurrence of annealing phenomenon, grain growth and precipitation dissolution in this zone [4,7,16].

A comparison between microhardness profile of cross section of A413/SiC<sub>p</sub> surface composite and A413/SiC<sub>p</sub>/MoS<sub>2p</sub> surface hybrid composite in the planes perpendicular to the FSP direction is also illustrated in Fig. 3. It is clear that the incorporation of MoS<sub>2</sub> lubricant particles in A413/SiC<sub>p</sub> surface composite results in the decrease of microhardness. This is due to the lower hardness of MoS<sub>2</sub> lubricant particles compared with SiC reinforcement particles, and lower fraction of SiC reinforcement particles in A413/SiC<sub>p</sub>/MoS<sub>2p</sub> surface hybrid composite rather than A413/SiC<sub>p</sub> surface composite. Figure 3 also illustrates that the microhardness of advancing side (AS) is higher than that of retreating side (RS). The more homogeneous distribution of particles and more fluidity amount of material in the AS leads to the increasing microhardness of AS compared with RS [11].

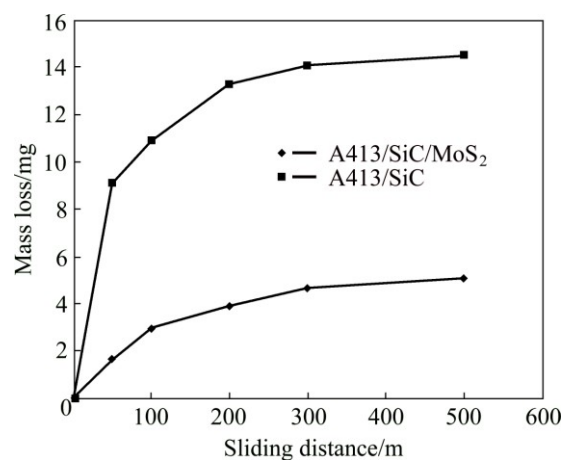
### 3.3 Wear resistance

Figure 4 shows the variations of friction coefficient versus sliding distance for A413/SiC<sub>p</sub> surface composite and A413/SiC<sub>p</sub>/MoS<sub>2p</sub> surface hybrid composite. This figure indicates that MoS<sub>2</sub> lubricant particles decrease the friction coefficient of A413/SiC<sub>p</sub> surface composite. Therefore, A413/SiC<sub>p</sub>/MoS<sub>2p</sub> surface hybrid composite has lower friction coefficient than A413/SiC<sub>p</sub> surface composite. The results showed that the average values of friction coefficient for A413/SiC<sub>p</sub> surface composite and A413/SiC<sub>p</sub>/MoS<sub>2p</sub> surface hybrid composite are 0.436 and 0.391, respectively. According to Fig. 4, there are large changes in the friction coefficient due to the periodical accumulation and elimination of wear debris on the worn surface and repeated banding structure in the tool traveling direction [4,18].

Figure 5 illustrates the relationship between mass loss and sliding distance for A413/SiC<sub>p</sub> surface composite and A413/SiC<sub>p</sub>/MoS<sub>2p</sub> surface hybrid composite. It is clear that the mass loss of A413/SiC<sub>p</sub>/MoS<sub>2p</sub> surface hybrid composite is lower than that of A413/SiC<sub>p</sub> surface composite. In fact, MoS<sub>2</sub> lubricant particles result in the decrease of mass loss of A413/SiC<sub>p</sub> surface composite. The results showed that



**Fig. 4** Variation of friction coefficient versus sliding distance for A413/SiC<sub>p</sub> surface composite (a) and A413/SiC<sub>p</sub>/MoS<sub>2p</sub> surface hybrid composite (b)



**Fig. 5** Relationship between mass loss and sliding distance for A413/SiC<sub>p</sub> surface composite and A413/SiC<sub>p</sub>/MoS<sub>2p</sub> surface hybrid composite

the maximum values of mass loss for A413/SiC<sub>p</sub> surface composite and A413/SiC<sub>p</sub>/MoS<sub>2p</sub> surface hybrid composite are 14.5 mg and 5.1 mg, respectively. According to Fig. 5, the mass loss curves of both samples in initial sliding stages show an increasing trend with increasing sliding distance, whereas, at long sliding distances, they approach a steady state condition with increasing sliding distance [4,8].

Therefore, the results reveal that MoS<sub>2</sub> lubricant particles lead to the decrease in friction coefficient and mass loss, and thus, result in the improvement of

tribological behavior.

The scanning electron microscopy was used to study the wear mechanisms of both samples. Figures 6 and 7 show the scanning electron micrographs of worn surfaces and wear debris, respectively, in different magnifications. As can be seen in Figs. 6 and 7, both samples exhibit comparatively same worn surfaces and wear debris which confirm that same wear mechanisms

exist in both samples. However, more damages are detectable on the worn surface of A413/SiC<sub>p</sub> surface composite than A413/SiC<sub>p</sub>/MoS<sub>2p</sub> surface hybrid composite.

As shown in Fig. 6, the heavy material removal, shallow parallel scratches and delamination effects are observed on the worn surfaces of both samples. The material removal and parallel scratches indicate adhesive

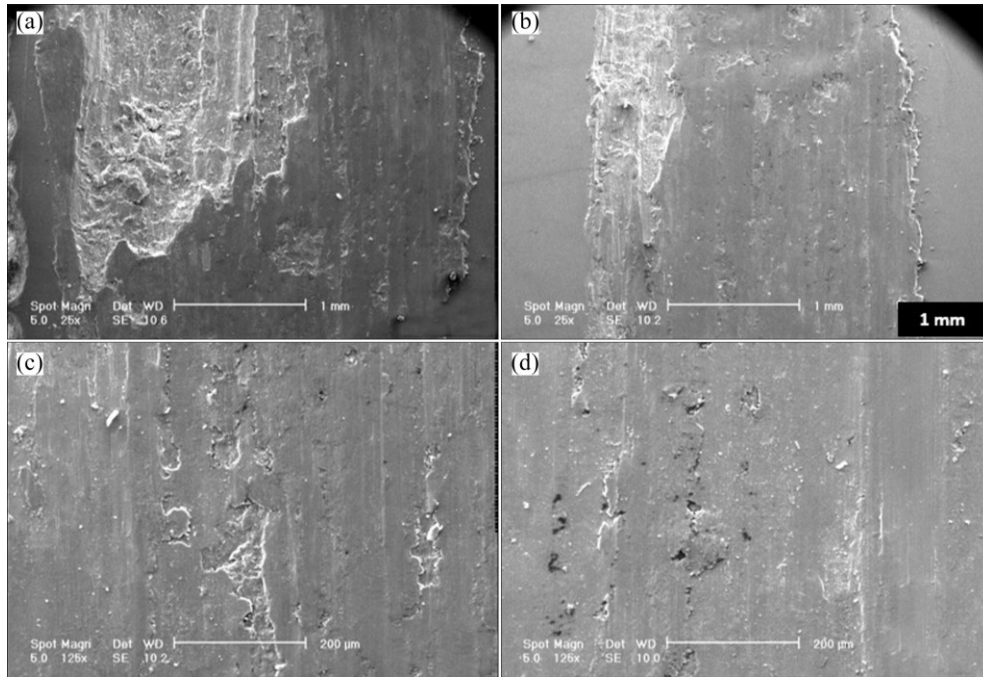


**Fig. 6** Scanning electron micrographs of worn surfaces of A413/SiC<sub>p</sub> surface composite (a, c) and A413/SiC<sub>p</sub>/MoS<sub>2p</sub> surface hybrid composite (b, d)

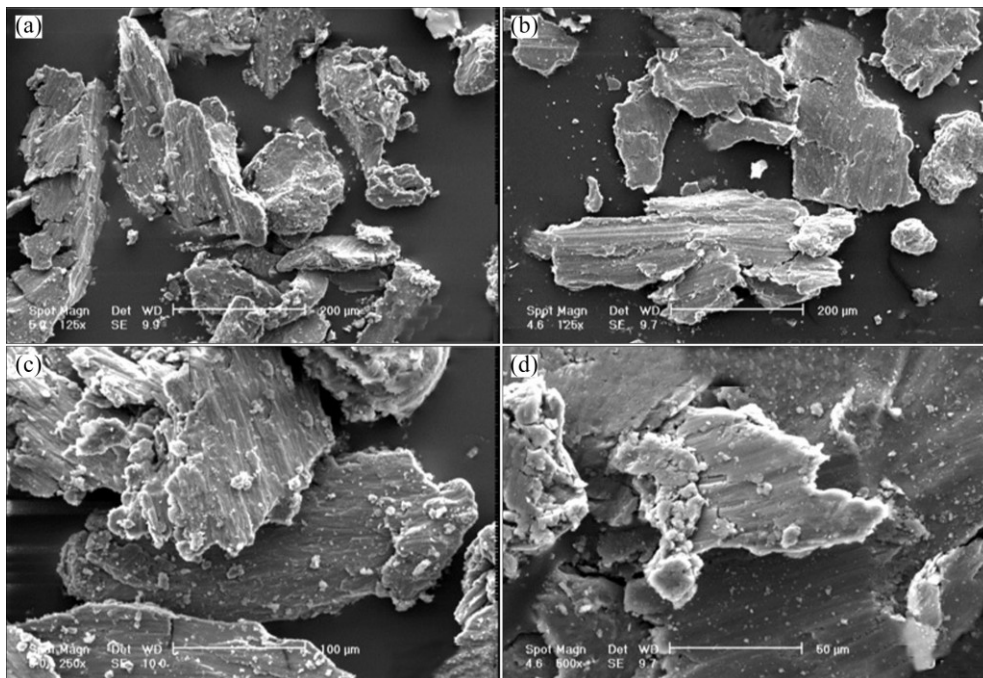


**Fig. 7** Scanning electron micrographs of wear debris of A413/SiC<sub>p</sub> surface composite (a, c) and A413/SiC<sub>p</sub>/MoS<sub>2p</sub> surface hybrid composite (b, d)

and abrasive wear mechanisms, respectively. ASHRAFI et al [19] used the following equation for the abrasive wear of ductile materials:

$$V = \alpha\beta \frac{WL}{H_v} \quad (1)$$

where  $V$  is the abrasive wear volume,  $W$  is the normal load,  $L$  is the sliding distance,  $H_v$  is the Vickers hardness, and  $\alpha$  and  $\beta$  are the constant factors of abrasive wear. According to this equation, the abrasive wear volume has inverse relationship with Vickers hardness value. Therefore, the presence of SiC reinforcement particles with high Vickers hardness results in the decrease of role of abrasive mechanism for both samples. In fact, the abrasive wear mechanism does not have an important role on the wear of both samples.

For further details of wear mechanism of both samples, the EDS analysis was applied. Table 2 shows the EDS results of worn surfaces for both samples. According to Table 2, the worn surfaces have Fe and O which indicate that a mechanically mixed layer (MML) has been formed on the worn surfaces of both samples. The presence of Fe and O in the EDS results is due to the steel pin and oxidation reaction, respectively. The generation of MML on the worn surface was also reported in many Al alloys such as A356 [8] and pure Al [19]. The fabrication of MML results in transferring the shear stresses and creating the micro cracks on the matrix surface underneath the MML, and then, the intersection of micro cracks leads to detaching the wear debris from the MML with plate shape by the delamination mechanism [8,19]. In fact, it seems that the formation and delamination of MML are predominant wear mechanisms of both samples. Nevertheless, there are lower surface damages and subsequently lower material removal in A413/SiC<sub>p</sub>/MoS<sub>2p</sub> surface hybrid composite compared with A413/SiC<sub>p</sub> surface composite. This is attributed to the presence of MoS<sub>2</sub> lubricant particles which leads to the decrease of shear stresses and reduction of micro cracks in the matrix surface underneath the MML of A413/SiC<sub>p</sub>/MoS<sub>2p</sub> surface hybrid composite [8]. In fact, the presence of MoS<sub>2</sub> lubricant particles in the MML improves the friction stability of A413/SiC<sub>p</sub>/MoS<sub>2p</sub> surface hybrid composite compared with A413/SiC<sub>p</sub> surface composite which is clear in Figs. 4 and 5. It is notable that although A413/SiC<sub>p</sub> surface composite has higher Vickers microhardness compared with A413/SiC<sub>p</sub>/MoS<sub>2p</sub> surface hybrid composite, the wear resistance of A413/SiC<sub>p</sub> surface composite is lower than that of A413/SiC<sub>p</sub>/MoS<sub>2p</sub> surface hybrid composite. In addition, the noise of wear test for A413/SiC<sub>p</sub>/MoS<sub>2p</sub> surface hybrid composite was lower than that of A413/SiC<sub>p</sub> surface composite. As mentioned above, these results are due to the generation of MML

containing MoS<sub>2</sub> lubricant particles on the worn surface of A413/SiC<sub>p</sub>/MoS<sub>2p</sub> surface hybrid composite.

**Table 2** EDS results of worn surfaces of surface composites

Surface composite	Mole fraction/%					
	Al	Si	Fe	O	Mo	S
A413/SiC <sub>p</sub>	30	16	30	23	–	–
A413/SiC <sub>p</sub> /MoS <sub>2p</sub>	26	13	18	11	24	7

As shown in Fig. 7, the wear debris of both sample have mainly two different morphologies: plate shape which suggests the delamination mechanism and stratified shape which indicates the adhesive mechanism. It is clear that more wear debris with stratified shape exist in A413/SiC<sub>p</sub> surface composite compared with A413/SiC<sub>p</sub>/MoS<sub>2p</sub> surface hybrid composite. Since the wear debris with stratified shape result from the adhesive mechanism, it can be concluded that more adhesive mechanism and subsequently more material removal occur in A413/SiC<sub>p</sub> surface composite rather than in A413/SiC<sub>p</sub>/MoS<sub>2p</sub> surface hybrid composite. This result is consistent with SEM images of worn surfaces. In fact, the generation of MML containing MoS<sub>2</sub> lubricant particles decreases the metal-to-metal contact and subsequently reduces the material removal for A413/SiC<sub>p</sub>/MoS<sub>2p</sub> surface hybrid composite. Furthermore, the existence of few fine particles in the wear debris shows that the abrasive mechanism does not have an important role on the wear of both samples.

## 4 Conclusions

1) A413/SiC<sub>p</sub> surface composite and A413/SiC<sub>p</sub>/MoS<sub>2p</sub> surface hybrid composite were successfully produced by FSP.

2) It is clear that during the fabrication of both samples, the FSP leads to the remarkable microstructural modification of Al matrix, and subsequently makes a uniform distribution of smaller broken silicon flakes and  $\alpha$ (Al) dendrites in the Al matrix.

3) A413/SiC<sub>p</sub>/MoS<sub>2p</sub> surface hybrid composite has a lower value of maximum microhardness as compared with A413/SiC<sub>p</sub> surface composite. This is due to the existence of MoS<sub>2</sub> particles with less hardness than SiC particles in A413/SiC<sub>p</sub>/MoS<sub>2p</sub> surface hybrid composite.

4) The friction coefficient and mass loss of A413/SiC<sub>p</sub>/MoS<sub>2p</sub> surface hybrid composite show lower values than A413/SiC<sub>p</sub> surface composite. This is due to the presence of MoS<sub>2</sub> particles acting as the solid lubricant elements in A413/SiC<sub>p</sub>/MoS<sub>2p</sub> surface hybrid composite.

5) The presence of shallow parallel scratches on the

worn surfaces and the existence of few fine particles in the wear debris show that the abrasive mechanism does not have an important role on the wear of both samples.

6) A mechanically mixed layer (MML) containing Fe and O was formed on the worn surfaces of both samples. The formation and delamination of MML are predominant wear mechanisms of both samples.

7) The presence of MoS<sub>2</sub> lubricant particles in the MML of A413/SiC<sub>p</sub>/MoS<sub>2p</sub> surface hybrid composite leads to decreasing the metal-to-metal contact and subsequently decreasing the adhesive mechanism in A413/SiC<sub>p</sub>/MoS<sub>2p</sub> surface hybrid composite compared with A413/SiC<sub>p</sub> surface composite.

## References

- [1] AMMAR H R, MOREAU C, SAMUEL A M, SAMUEL F H, DOTY H W. Influences of alloying elements, solution treatment time and quenching media on quality indices of 413-type Al–Si casting alloys [J]. *Materials Science and Engineering A*, 2008, 489: 426–438.
- [2] MAHMOUD T S, MOHAMED S S. Improvement of microstructural, mechanical and tribological characteristics of A413 cast Al alloys using friction stir processing [J]. *Materials Science and Engineering A*, 2012, 558: 502–509.
- [3] MISHRA R S, MA Z Y. Friction stir welding and processing [J]. *Materials Science and Engineering R*, 2005, 50: 1–78.
- [4] ZAHMATKESH B, ENAYATI M H, KARIMZADEH F. Tribological and microstructural evaluation of friction stir processed Al2024 alloy [J]. *Materials and Design*, 2010, 31: 4891–4896.
- [5] CHOI D H, KIM Y H, AHN B W, KIM Y I, JUNG S B. Microstructure and mechanical property of A356 based composite by friction stir processing [J]. *Transactions of Nonferrous Metals Society of China*, 2013, 23: 335–340.
- [6] SARKARI KHORRAMI M, KAZEMINEZHAD M, KOKABI A H. The effect of SiC nanoparticles on the friction stir processing of severely deformed aluminum [J]. *Materials Science and Engineering A*, 2014, 602: 110–118.
- [7] MAZAHERI Y, KARIMZADEH F, ENAYATI M H. A novel technique for development of A356/Al<sub>2</sub>O<sub>3</sub> surface nanocomposite by friction stir processing [J]. *Journal of Materials Processing Technology*, 2011, 211: 1614–1619.
- [8] ALIDOKHT S A, ABDOLLAH-ZADEH A, SOLEYMANI S, ASSADI H. Microstructure and tribological performance of an aluminum alloy based hybrid composite produced by friction stir processing [J]. *Materials and Design*, 2011, 32: 2727–2733.
- [9] DEVARAJU A, KUMAR A, KUMARASWAMY A, KOTIVEERACHARI B. Wear and mechanical properties of 6061-T6 aluminum alloy surface hybrid composites [(SiC+Gr) and (SiC+Al<sub>2</sub>O<sub>3</sub>)] fabricated by friction stir processing [J]. *Journal of Materials Research and Technology*, 2013, 2(4): 362–369.
- [10] DEVARAJU A, KUMAR A, KOTIVEERACHARI B. Influence of addition of Grp/Al<sub>2</sub>O<sub>3p</sub> with SiCp on wear properties of aluminum alloy 6061-T6 hybrid composites via friction stir processing [J]. *Transactions of Nonferrous Metals Society of China*, 2013, 23: 1275–1280.
- [11] AKRAMIFARD H R, SHAMANIAN M, SABBAGHIAN M, ESMAILZADEH M. Microstructure and mechanical properties of Cu/SiC metal matrix composite fabricated via friction stir processing [J]. *Materials and Design*, 2014, 54: 838–844.
- [12] AL-SAMARAI R A, HAFTIRMAN, AHMAD K R, AL-DOURI Y. Effect of load and sliding speed on wear and friction of aluminum–silicon casting alloy [J]. *International Journal of Scientific and Research Publications*, 2012, 16(4): 1–4.
- [13] GAN Wen-ying, ZHOU Zheng, ZHANG Hang, PENG Tao. Evolution of microstructure and hardness of aluminum after friction stir processing [J]. *Transactions of Nonferrous Metals Society of China*, 2014, 24: 975–981.
- [14] DOLATKHAH A, GOLBABAIE P, BESHARATI GIVI M K, MOLAEKIYA F. Investigating effects of process parameters on microstructural and mechanical properties of Al5052/SiC metal matrix composite fabricated via friction stir processing [J]. *Materials and Design*, 2012, 37: 458–464.
- [15] EL-RAYES M M, EL-DANAF E A. The influence of multi-pass friction stir processing on the microstructural and mechanical properties of aluminum alloy 6082 [J]. *Journal of Materials Processing Technology*, 2012, 212: 1157–1168.
- [16] SABBAGHIAN M, SHAMANIAN M, AKRAMIFARD H R, ESMAILZADEH M. Effect of friction stir processing on the microstructure and mechanical properties of Cu–TiC composite [J]. *Ceramics International*, 2014, 40: 12969–12976.
- [17] SALEHI M, FARNOUSH H, AGHAZADEH MOHANDESI J. Fabrication and characterization of functionally graded Al–SiC nanocomposite by using a novel multistep friction stir processing [J]. *Materials and Design*, 2014, 63: 419–426.
- [18] ANVARI S R, KARIMZADEH F, ENAYATI M H. Wear characteristics of Al–Cr–O surface nano-composite layer fabricated on Al6061 plate by friction stir processing [J]. *Wear*, 2013, 304: 144–151.
- [19] ASHRAFI H, ENAYATI M H, EMADI R. Tribological Properties of nanostructured Al/Al<sub>12</sub>(Fe,V)<sub>3</sub>Si Alloys [J]. *Acta Metallurgica Sinica (English Letters)*, 2015, 28(1): 83–92.

# 采用 MoS<sub>2</sub> 润滑颗粒提高搅拌摩擦制备 A413/SiC<sub>p</sub> 表面复合材料的摩擦性能

M. JANBOZORGI<sup>1</sup>, M. SHAMANIAN<sup>2</sup>, M. SADEGHIAN<sup>1</sup>, P. SEPEHRINIA<sup>2</sup>

1. Department of Materials Science and Engineering, Sharif University of Technology, Tehran 1136511155, Iran;
2. Department of Materials Science and Engineering, Isfahan University of Technology, Isfahan 8415683111, Iran

**摘要:** 研究 MoS<sub>2</sub> 润滑颗粒对搅拌摩擦制备 A413/SiC<sub>p</sub> 表面复合材料显微组织、显微硬度和摩擦性能的影响。在模具转速为 1600 r/min, 模具行进速率为 25 mm/min, 模具倾角为 3°条件下进行单道次摩擦搅拌。采用光学显微镜、电子扫描显微镜、显微硬度和往复磨损实验对材料进行表征。结果表明, 在 A413/SiC<sub>p</sub> 表面复合材料中添加 MoS<sub>2</sub> 润滑颗粒可减小摩擦因数和质量损失。在 A413/SiC<sub>p</sub>/MoS<sub>2p</sub> 表面复合材料中, 可形成含 MoS<sub>2</sub> 润滑颗粒的机械混合层, 使金属与金属间的接触减小, 进而提高材料的摩擦性能。

**关键词:** 搅拌摩擦工艺; 表面混合复合材料; 显微组织; 显微硬度; 摩擦性能

(Edited by Yun-bin HE)